Spin-dependent band structure, Fermi surface, and carrier lifetime of permalloy

D. Y. Petrovykh, K. N. Altmann, H. Höchst,[a] M. Laubscher, S. Maat,[b] G. J. Mankey,[b] and F. J. Himpsel[c]
Department of Physics, University of Wisconsin Madison, 1150 University Ave., Madison, Wisconsin 53706-1390

Angle-resolved photoemission is used to determine the energy bands of permalloy ($Ni_{0.8}Fe_{0.2}$) and compare them to Ni, Co, and Cu. The energy and momentum resolution (≈ 0.01 eV and ≈ 0.01 Å^{-1}) is high enough to resolve the magnetically split bands at the Fermi level that are responsible for spin-dependent conductivity and tunneling. For the Σ_1 band we find the magnetic exchange splittings $\delta E_{ex} = 0.27$ eV (0.23 eV for Ni), $\delta k_{ex} = 0.16 \pm 0.02$ Å^{-1} (0.12 ± 0.01 Å^{-1} for Ni), the Fermi velocity $v_{F\uparrow} = (0.22 \pm 0.02)10^6$ m/s (0.28×10^6 m/s for Ni, 0.33×10^6 m/s for fcc Co), and the widths $\delta k_\uparrow \leq 0.11$ Å^{-1} and $\delta k_\downarrow = 0.24$ Å^{-1}. Compared to Ni, permalloy features a 27% larger magnetic splitting of the Fermi surface and an extremely short mean free path of 4–8 Å for minority spins. © *1998 American Institute of Physics.* [S0003-6951(98)01249-2]

Permalloy is one of the most common materials in magnetic data storage and can be found in a variety of magnetic micro- and nanostructures.[1] Several useful properties come together to make permalloy so pervasive: The magnetostriction of Ni–Fe alloys vanishes at the composition of permalloy ($Ni_{0.8}Fe_{0.2}$), keeping the strain in small structures from magnetizing the material. High permeability and low coercivity make permalloy an excellent soft magnet and provide low switching fields in sensors. State-of-the-art reading heads for hard disks utilize the anisotropic magnetoresistance (AMR) of permalloy, or the giant magnetoresistance (GMR) of permalloy/Cu/Co films. Particularly remarkable is the large difference in conductivity of majority and minority spins in permalloy.[2,3] Most recently, it is being studied in the context of spin-polarized tunneling for a nonvolatile, magnetic random access memory (MRAM). Surprisingly, it emits electrons with a higher spin polarization (45%) than pure Fe and Ni (40% and 23%–33%),[4] even though its magnetic moment is lower than that of Fe.

Despite this rich spectrum of magnetic phenomena and applications, very little is known about the underlying electronic structure. To our knowledge, the energy bands of permalloy have not been mapped yet, despite extensive work on Ni.[5–7] Calculations of magnetic energy bands[8,9] are not as reliable as one might expect. For example, the magnetic splitting of the d bands in Ni is overestimated by a factor of 2 to 3 in first principles, local density calculations, and the calculated band width is 40% too large.[5] Fermi surface techniques, such as the de Haas van Alphen effect,[8] are difficult in alloys because of the reduced mean free path. Even beyond the specific case of permalloy, basic concepts about the band structure of alloys[10] can be tested. Is there a common band structure, or a separate set of levels for each of the constituents? In permalloy, one might speculate that the de-

localized s,p electrons form a common band, whereas the localized d electrons produce a Fe impurity level separated from the Ni d levels. There has been a long-standing discussion about the electrons that are responsible for spin transport in $3d$ transition metals.[1,11] They are crucial for magnetic devices such as the spin valve, the spin transistor, and the magnetic tunnel junction. The $3d$ electrons carry a large magnetization and a high density of states, compensated by a low group velocity. The s,p electrons have a large group velocity but low density. A possible solution of this dilemma has been the notion of an ''itinerant d band'' that exhibits magnetism as well as conductivity.[11]

We use high resolution photoelectron spectroscopy to map out the energy band dispersion and lifetime broadening of electrons close to the Fermi level E_F. This technique has advanced in recent years to achieve energy resolutions better than the thermal energy kT, even for low temperatures. That makes the electrons at E_F which are responsible for conductivity, magnetoresistance, and spin-polarized tunneling accessible. Our focus lies on the region where the so-called ''s,p band'' crosses E_F and flattens out to become d like. At this point, we find both, a sizable magnetic splitting and a substantial group velocity, suggesting that this part of the Fermi surface represents the itinerant d band. In addition, we are able to resolve the energy and momentum broadening caused by the finite lifetime and mean free path of electrons near E_F, which brings our data into contact with spin transport measurements in GMR structures. The salient features of our results are a 27% larger magnetic splitting of the Fermi surface compared to Ni, and a much shorter minority spin lifetime at E_F, which produces a mean free path of only 4–8 Å.

Permalloy was grown epitaxially on a Ni(100) surface in order to minimize lattice mismatch ($\approx 0.7\%$) and to have a direct comparison with the Ni band structure under exactly the same conditions. The permalloy film was about 10 monolayers (35 Å) thick, which exceeds the escape depth of the photoelectrons. The stoichiometry was monitored by photoemission from the Fe $3p$ and Ni $3p$ core levels.[12] The films were deposited below room temperature (100–200 K) to pre-
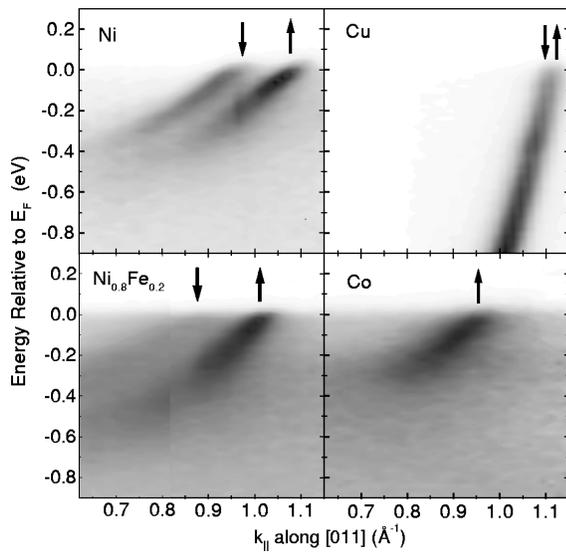
FIG. 1. Energy and momentum distribution of photoelectrons near the Fermi level crossing of the Σ_1 band, obtained with a two-dimensional photoelectron detector (high photoelectron intensity is dark). The four panels display data from the (100) surface of permalloy ($Ni_{0.8}Fe_{0.2}$), Ni, Cu, and fcc Co. For Ni, the spin splitting of the Σ_1 band is clearly visible, for permalloy the minority spin component is much weaker. In Co, the minority spin Σ_1 band never reaches below E_F.
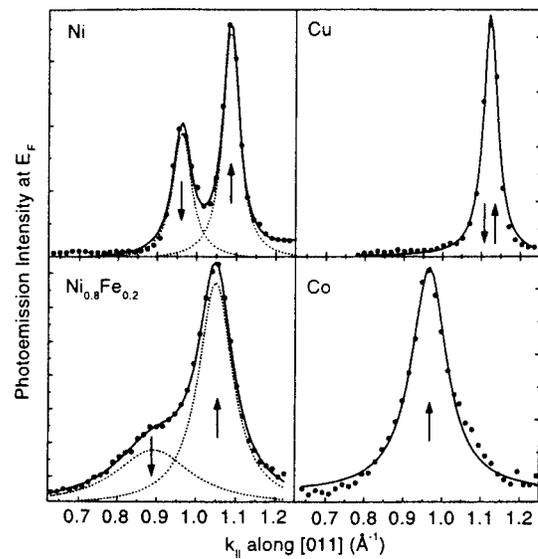
FIG. 2. Momentum distribution of photoelectrons at E_F (horizontal cut in Fig. 1). The maxima give the Fermi wave vectors k_F and the spin splitting $\delta k_{ex} = k_{F\uparrow} - k_{F\downarrow}$. The width δk of the Lorentzian fit curves can be used to derive the mean free path $\lambda = 1/\delta k$. Note the large width of the minority peak in permalloy, which translates into $\lambda_\downarrow = 4$ Å.

vent island formation. A postanneal to 500–700 K sharpened the photoemission features. Anneals higher than ≈ 800 K caused Ni-rich films. For comparison, we also prepared a Cu(100) single crystal and grew an epitaxial fcc Co(100) film, 10 monolayers thick. Angle-resolved photoelectron spectra were taken at ≈ 100 K with an energy resolution of 9 meV (photons+electrons), using a new undulator beam line at the SRC and a Scienta spectrometer. The angular dependence was determined by parallel detection over a $14°$ range with $\pm 0.15°$ (≈ 0.01 Å^{-1}) resolution. Photons were incident at $50°$ from the emitted electrons with an in-plane electric field vector. This geometry selects even states, such as the *s,p* band.

Among the large volume in **k**-space sampled in this experiment, only a small portion is represented in Figs. 1–3.[13] It contains the Fermi level crossing of the Σ_1 *s* and *p* bands along a [011] line starting from the (200) Γ point. The **k** vector is determined following standard procedures. The parallel component $k^\parallel$ is given by the kinetic energy E_{kin} and the polar angle ϑ via $k^\parallel = \hbar^{-1} (2mE_{kin})^{1/2} \sin \vartheta$. The perpendicular component $k^\perp$ is obtained from E_{kin} via a free electron final state band (fine circles in Fig. 4). As a test of our method, we determine the Fermi vector k_F and the Fermi velocity $v_F = \hbar^{-1} \partial E/\partial k$ of Cu from Fig. 1. The values are consistent with de Haas van Alphen data ($k_F = 1.23$ Å^{-1}, $v_F = 1.10 \times 10^6$ m/s). In Cu, the Fermi velocity is comparable to the free electron value of 1.58×10^6 m/s. In the transition metals Ni, permalloy, and Co, it is four times smaller ($v_F = 0.28$, 0.22, and 0.33×10^6 m/s, rsp.)[14] The steep *s,p* band begins to hybridize with the flat *d* bands at the Fermi level. However, v_F is still three times as large as the average velocity $\langle v \rangle = 0.1 \times 10^6$ m/s of the *d*-like stretch of the Σ_1 band (from k_F to $\Gamma_{12} = E_F - 0.6$ eV).

A ferromagnetic exchange splitting of the Σ_1 band is clearly visible in Fig. 1 for Ni. In permalloy, the minority

spin component is hard to discern, because it is much broader and weaker. It can be observed more clearly in Fig. 2, where a sharp majority spin Fermi level crossing is located next to a broad minority spin crossing. The *k* splitting in Fig. 2 is $\delta k_{ex} = 0.16$ Å^{-1} in permalloy and $\delta k_{ex} = 0.12$ Å^{-1} in Ni. The energy splitting in Fig. 3 is $\delta E_{ex} = 0.27$ eV in permalloy and $\delta E_{ex} = 0.23$ eV in Ni, which is comparable to the splitting of the *d* bands in Ni.[5] The larger magnetic splitting of permalloy reflects its increased magnetic moment[15] (1.0 μ_B vs 0.6 μ_B in Ni), following a general trend[16] in 3*d* transition metals. In Co, the magnetic splitting is so large that the minority spin Σ_1 band moves up beyond E_F.[1,6]

The intensity of the majority peak at E_F is larger than that of the minority peak (Fig. 2), giving an area ratio of $A_\uparrow/A_\downarrow = 1.8$ in Ni and $A_\uparrow/A_\downarrow = 2.0$ in permalloy. It is inter-
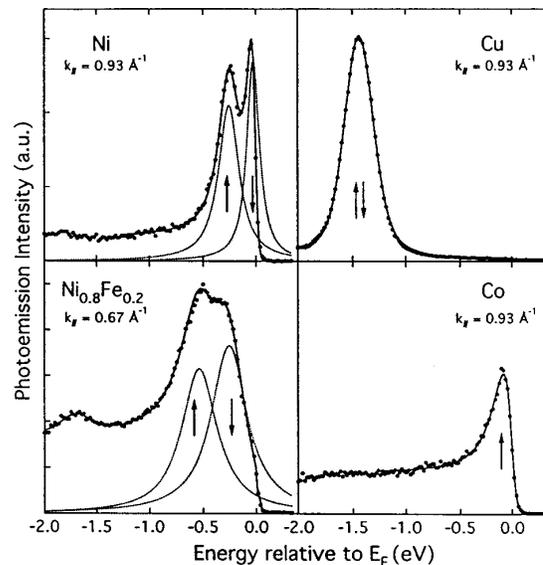
FIG. 3. Energy distributions of photoelectrons (vertical cuts in Fig. 1). The momentum $\mathbf{k}^\parallel$ has been chosen close to the Fermi level crossing in the [011] direction. In cobalt the minority band lies above E_F.
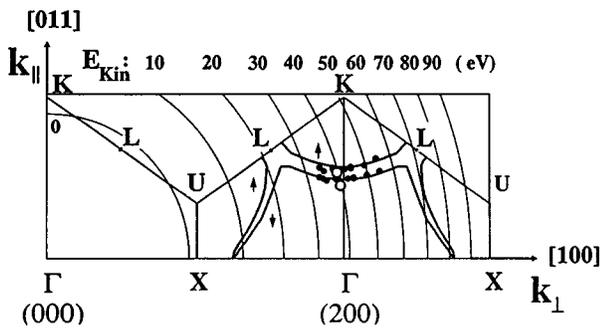
Appl. Phys. Lett., Vol. 73, No. 23, 7 December 1998

Petrovykh et al.   3461

FIG. 4. Spin-split Fermi surface of the *s,p* band in Ni and permalloy (full and open circles), obtained from photoemission data similar to Fig. 2 at various photon energies. The fat lines are calculated from the experimental bulk bands of Ni.

esting to note that the spin polarization $P=(A_\uparrow-A_\downarrow)/(A_\uparrow+A_\downarrow)$ derived from these areas is not too far from the experimental values P_{tunnel} from spin-polarized tunneling ($P=29\%$ versus $P_{tunnel}=23\%-33\%$ in Ni, $P=33\%$ vs $P_{tunnel}=45\%$ in permalloy). A common model of spin-polarized tunneling[11] predicts a polarization $P_{model}=(k_{F\uparrow}-k_{F\downarrow})/(k_{F\uparrow}+k_{F\downarrow})$, which comes out too small for Ni (6% from our k_F, 5%, 7% from de Haas van Alphen data),[8] as well as for permalloy (8% from our k_F). Thus, photoemission might provide a clue for establishing a better model of spin-polarized tunneling.

Figure 1 makes it clear that the bands quickly become broader when moving away from E_F. The broadening is mostly due to the reduced lifetime τ for energies below E_F, where more combinations for decay by electron-electron scattering become accessible. The lifetime broadening is $\delta E=\hbar\,\delta\omega=\hbar/\tau$ (full width half maximum of a Lorentzian). The energy broadening leads to a k broadening via $\delta E=\partial E/\partial k\,\delta k=\hbar v_F\delta k$. The k-broadening δk, in turn, gives rise to a finite mean free path $\lambda=1/\delta k$. A residual k broadening is found at E_F (Fig. 2). It can be accounted for by finite momentum and energy resolution, structural and thermal disorder, intrinsic disorder in a random alloy, and lifetime broadening in the initial and final state. These phenomena can explain the observed $\delta k=0.04$ Å^{-1} in Cu and $\delta k_\uparrow=\delta k_\downarrow=0.05$ Å^{-1} in Ni, and possibly $\delta k_\uparrow=0.12$ Å^{-1} in fcc Co. In permalloy, however, δk is spin dependent ($\delta k_\downarrow=0.24$ Å^{-1} vs $\delta k_\uparrow=0.11$ Å^{-1}). That suggests a lifetime contribution of 0.13–0.24 Å^{-1}, with minority spins living shorter than majority spins. This is to be explained by an argument used in the analysis of GMR structures.[1,3] The majority spin d bands are completely filled, as in a noble metal. Only s,p states remain available for scattering, and the lifetime increases. The minority spin bands keep the characteristics of a transition metal, that is a high density of d states at E_F that provides scatterers for minority spin s,p electrons. Our lifetime broadening of $0.13\leqslant\delta k\leqslant0.24$ Å^{-1} leads to a mean free path of $4\leqslant\lambda_\downarrow\leqslant8$ Å. This value is consistent with results from GMR structures[3] ($\lambda_\downarrow\leqslant6$ Å at room temperature, 10 Å at 4 K, 6 Å at 1.5 K). Determining the mean free path from the momentum broadening makes it possible to extend transport measurements to shorter λ values where GMR structures would require atomically perfect interfaces.

The Fermi surface can be mapped out by measuring Fermi level crossings analogous to Figs. 1 and 2 over a range

of photon energies. The resulting data points in Fig. 4 fall onto the spin-split *sp* sheet.[8,17] The most notable change from Ni to permalloy is a 27% larger magnetic splitting of the Fermi surface.

In summary, we have mapped out the energy bands of permalloy for the first time and have demonstrated how high-resolution photoemission near the Fermi level helps explaining magnetic and transport phenomena in terms of the underlying band structure. There exist many other interesting magnetic alloys, such as invar,[18] where our method is directly applicable.

[1] For reviews, see Phys. Today **48**, 24 (1995); F. J. Himpsel, J. E. Ortega, G. J. Mankey, and R. F. Willis, Adv. Phys. **47**, 511 (1998).

[2] D. M. C. Nicholson, W. H. Butler, W. A. Shelton, Y. Wang, X.-G. Zhang, G. M. Stocks, and J. M. MacLaren, J. Appl. Phys. **81**, 4023 (1997).

[3] B. Dieny, Europhys. Lett. **17**, 261 (1992); B. A. Gurney, V. S. Speriosu, J. P. Nozieres, H. Lefakis, D. R. Wilhoit, and O. U. Need, Phys. Rev. Lett. **71**, 4023 (1993); B. Dieny, A. Granovsky, A. Vedyaev, N. Ryzhanova, C. Cowache, and L. G. Pereira, J. Magn. Magn. Mater. **151**, 378 (1995); W. P. Pratt, Q. Yang, L. L. Henry, P. Holody, W.-C. Chiang, P. A. Schroeder, and J. Bass, J. Appl. Phys. **79**, 5811 (1996).

[4] R. Meservey and P. M. Tedrow, Phys. Rep. **238**, 173 (1994); J. S. Moodera and R. J. M. van de Veerdonk (unpublished).

[5] D. E. Eastman, F. J. Himpsel, and J. A. Knapp, Phys. Rev. Lett. **40**, 1514 (1978); F. J. Himpsel, J. A. Knapp, and D. E. Eastman, Phys. Rev. B **19**, 2919 (1979); W. Eberhardt and E. W. Plummer, Phys. Rev. B **21**, 3245 (1980); P. Heimann, F. J. Himpsel, and D. E. Eastman, Solid State Commun. **39**, 219 (1981).

[6] G. J. Mankey, R. F. Willis, and F. J. Himpsel, Phys. Rev. B **48**, 10 284 (1993).

[7] P. Aebi, T. J. Kreutz, J. Osterwalder, R. Fasel, P. Schwaller, and L. Schlapbach, Phys. Rev. Lett. **76**, 1150 (1996); G. J. Mankey, K. Subramanian, R. L. Stockbauer, and R. L. Kurtz, Phys. Rev. Lett. **78**, 1146 (1997); T. J. Kreutz, T. Greber, P. Aebi, and J. Osterwalder, Phys. Rev. B **58**, 1300 (1998).

[8] First principles band calculation for Ni: C. S. Wang and J. Callaway, Phys. Rev. B **15**, 298 (1977); Fermi surface of Ni: D. C. Tsui, Phys. Rev. **164**, 669 (1967); A. V. Gold, J. Low Temp. Phys. **16**, 3 (1974).

[9] Calculation for permalloy: Ph. Lambin and F. Herman, Phys. Rev. B **30**, 6903 (1984); Compare also Ni₃Fe: M. C. Desjonquères and M. Lavagna, J. Phys. F **9**, 1733 (1979).

[10] B. L. Gyorffy, G. M. Stocks, W. M. Temmerman, R. Jordan, D. R. Lloyd, C. M. Quinn, and N. V. Richardson, Solid State Commun. **23**, 637 (1977).

[11] M. B. Stearns, J. Magn. Magn. Mater. **5**, 167 (1977); Phys. Today **34**, (1978).

[12] The Fe/Ni ratio was determined from the Fe 3p/Ni 3p area ratio, including minor corrections for the cross section ratio and for the energy-dependent transmission of the spectrometer. See also K. Wandlet and G. Ertl, J. Phys. F **6**, 1607 (1976).

[13] The data in Figs. 1–3 were taken at a photon energy $h\nu=44$ eV for permalloy and Ni, and at $h\nu=50$ eV for Cu and Co.

[14] The Fermi velocity was determined from peaks in k distributions at fixed energies similar to Fig. 2 with an accuracy of 0.02×10^6 m/s.

[15] H. Hasegawa and J. Kanamori, J. Phys. Soc. Jpn. **33**, 1599 (1972) and references therein; J. W. Cable and E. O. Wollan, Phys. Rev. B **7**, 2005 (1973).

[16] F. J. Himpsel, Phys. Rev. Lett. **67**, 2363 (1991).

[17] The Fermi surface is calculated from the experimental bulk bands, fitted by an empirical band calculation (see Refs. 1 and 4).

[18] F. O. Schumann, R. F. Willis, K. G. Goodman, and J. G. Tobin, Phys. Rev. Lett. **79**, 5166 (1997).